

Title	Carrier injection mechanism at the metal-semiconductor interface in CNT-FETs
Author(s)	SHIH, Hong-An
Citation	
Issue Date	2010-09
Type	Thesis or Dissertation
Text version	none
URL	<a href="http://hdl.handle.net/10119/9138">http://hdl.handle.net/10119/9138</a>
Rights	
Description	Assoc. Prof. Toshi-kazu SUZUKI, マテリアルサイエンス研究科, 修士

# Carrier injection mechanism at the metal-semiconductor interface in CNT-FETs

SHIH, Hong-An (Suzuki Laboratory)

## Introduction

Carbon nanotube (CNT) is a one-dimensional (1D) nanostructure material that offers superior electron transport properties by nature. The reduced phase space for scattering events in CNTs decreases the probability of scattering events and results in improved electrical characteristics. For that reason, CNT field effect transistors (CNT-FETs) is one of the most anticipated CNT-based applications in recent decades. Despite the tremendous progress in the device fabrication [1,2], understanding of carrier injection mechanism at the Schottky barrier (SB) formed by 1D CNT and three-dimensional (3D) metal remains incomplete. In order to truly harness the potential of this nanostructure, fundamental understanding of the basic physics that governs their behavior is necessary.

Current injection is a complicated subject especially when it comes to Schottky barrier type transistors. The thermally excited current from thermionic emission (TE) is directly related to temperature and SB height while the tunneling current from field emission (FE) is more concerned with the SB width modulation by gate voltage ( $V_{GS}$ ) and bias voltage ( $V_{DS}$ ) induced electric field. It was reported that the complete description on the operation of CNT-FET is usually the combination of both mechanisms, i.e., the thermally assisted tunneling through modulated Schottky barrier by electric field [3]. The question is how these two mechanisms link to each other, that is, the temperature or field strength by which one or the other becomes dominant is still unclear.

In this study, we focus on the details of current injection from a 3D metal into a 1D semiconducting CNT in a CNT-FET device. The analysis is based on  $I$ - $V$  characteristics by probe measurement with temperature range from 77 K to 393 K in order to collect comprehensive data on both thermally induced current at high-temperature/low-field and tunneling current at low-temperature/high-field. The CNT-FET device studied was fabricated by direct growth method which grows CNTs directly between source and drain electrodes. Out of the many devices fabricated, the one with single CNT bridging the electrodes was chosen for analysis.

## Device fabrication

In this study, a back-gate configuration device was fabricated on a p-type thermally oxidized Si/SiO<sub>2</sub> substrate where the SiO<sub>2</sub> layer acted as the gate insulator as shown in Fig. 1. Photolithography was employed in patterning the device structure of mass quantity. After development process, Molybdenum (Mo) layer of 100 nm was carried out in a technique called angle-deposition that allows the 2<sup>nd</sup> layer, cobalt (Co) of 2 nm, to settle on the adjacent area of Mo layer and substrate. This is necessary as Co acts as catalyst particle in the latter CNT synthesis process.

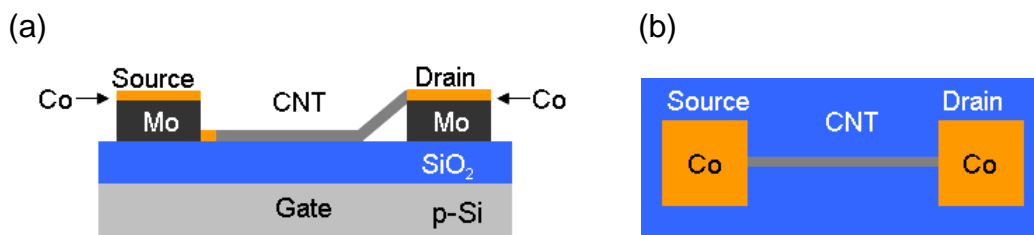


Fig. 1. CNT-FET device structure: (a) cross-sectional view, (b) top view.

Following electrode fabrication, alcohol catalytic chemical vapor deposition method using ethanol as the source material was employed to synthesize CNTs between the source and drain electrodes. Cobalt layer was first annealed at 900°C to form catalyst particles as the growth sites for CNTs. Ethanol gas was introduced and became carbon source in CNT self-assembly process upon its decomposition by heat. CNT bridged between source and drain electrodes were confirmed by SEM and Raman spectroscopy.

## Device Characteristics

$I$ - $V$  characteristics of CNT-FETs were investigated by changing bias voltages, drain-source voltage ( $V_{DS}$ ) and gate-source voltage ( $V_{GS}$ ), in temperature range 77-393K. The electrode symmetry was then evaluated using the  $I_D$  mapping. Figure 2 is the  $I_D$  mapping at 77 K, the solid and dashed line represent a symmetric current pair. It is evident enough to say the source and drain electrodes are symmetric as the solid and dashed line covered current region of almost identical order.

Among the possible carrier injection mechanisms, the thermionic emission (TE) theory was selected based on the experimental result obtained

above 300 K. Thermionic current for 3D metal and 1D semiconductor was derived and given by

$$I(T) = AT \exp\left(-\frac{\phi}{kT}\right), \quad (1)$$

where  $A = 2qk/h = 2.1 \times 10^{-8} \text{ A/K}$  ( $q$ : electron charge,  $k$ : Boltzman constant,  $h$ : Planck constant) and  $\phi$  is the Schottky barrier height. We calculated  $A$  and  $\phi$  by fitting the experimental data to this formula. However, as shown in Fig. 3, there is a correlation between  $A$  and  $\phi$ ;  $A$  is not constant and  $\phi$  takes negative values, indicating that the simple TE current cannot explain the experimental results.

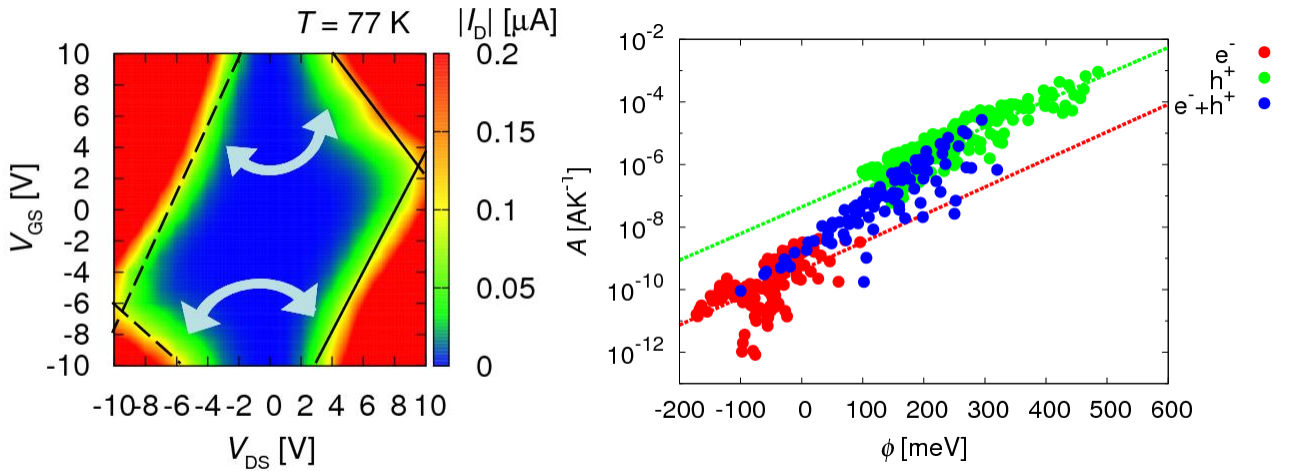


Fig. 2.  $I_D$  mapping at 77 K.

Fig. 3.  $A$ - $\phi$  plot.

A new formula was constructed with more complicated temperature term inside the exponential component. It has the following form,

$$I(T) = A_0 T \exp\left(-\frac{\phi_0}{kT} + \frac{a}{T^m}\right), \quad (2)$$

where  $\phi_0$  is the intrinsic Schottky barrier height and  $a$  is a function of electric field. With some algorithm manipulation, the equals is transformed into

$$I(T) \cong A_0 \exp\left[\frac{a(1-m)}{T_0^m}\right] T \exp\left[-\frac{1}{kT}\left(\phi_0 - \frac{akm}{T_0^{m-1}}\right)\right], \quad (3)$$

where  $T_0$  is the average measurement temperature. Eq. (3) can be related to Eq. (1) by following equations,

$$A = A_0 \exp\left[\frac{a(1-m)}{T_0^m}\right], \quad (4)$$

$$\phi = \phi_0 - \frac{akm}{T_0^{m-1}}, \quad (5)$$

$$\ln A = \left[ \ln A_0 + \frac{(1-m)\phi_0}{m kT_0} \right] - \frac{(1-m)\phi}{m kT_0}. \quad (6)$$

From Eq. (5), the negative  $\phi$  values is reasonable if  $a(F)$  is sufficiently large. The exponential relation between  $A$  and  $\phi$  can also be explained by Eq. (6). The index number of new temperature term is the gradient of  $A$ - $\phi$  fitting as shown by Eq. (6) and in Fig. 3. Both the electron and hole carriers yield the same order of magnitude for  $T$  term,  $m=3$ , Eq. (2) becomes

$$I(T) = A_0 T \exp\left(-\frac{\phi_0}{kT} + \frac{a}{T^3}\right). \quad (7)$$

It is interesting to notice the resemblance between the proposed formula in Eq. (7) and the conventional 3D-3D TFE formula. The index number of temperature term in both formulas are 3, more intriguingly, this number was obtained from experiment data.

Through Eq. (5), there is other important information hidden in the  $A$ - $\phi$  plot in Fig. 3. The intrinsic Schottky barriers height,  $\phi_0$ , for electron and hole carriers are the maximum  $\phi$  value indicated in  $A$ - $\phi$  plot if they can be specified. The intrinsic SB height for electron,  $\phi_{0n}$ , is  $\sim 0.1$  eV, and for holes,  $\phi_{0p}$ , is  $\sim 0.5$  eV. The bandgap for the CNT in this specific device studied is  $\sim 0.6$  eV. The band structure is illustrated in Fig. 4. This value also matches that obtained by Raman spectroscopy.

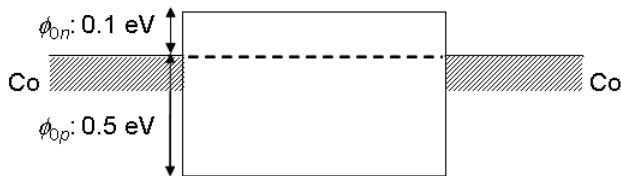


Fig. 4. Band structure of CNT in the device studied.

With the in-depth analysis carried out in this study, we were able to conclude the operation of CNT-FETs is dominated by thermionic field emission even at temperature above 300 K. Pure thermally induced current may only exist at low field limit even at this temperature range. The SB barrier structure modulated by electric field determines the probability of thermally assisted

tunneling. This mechanism governs the carrier injection behaviors from metal to CNT in CNT-FETs.

### **Reference**

- [1] S. J. Tans, M. H. Devoret, H. Dai, A. Thess, R. E. Smalley, L. J. Geerligs and C. Dekker: "Individual single-wall carbon nanotubes as quantum wires", *Nature* **386**(3) (1997) 474-477.
- [2] P. Avouris, P. Appenzeller, J. Martel, R. Wind, T. J. Watson: "Carbon Nanotube Electronics", *Procs of The IEEE*, **91**(11) (2003) 1772-1784.
- [3] S. Heinze, J. Tersoff, R. Martel, V. Derycke, J. Appenzeller, and Ph. Avouris, *Phys. Rev. Lett.* **89**, 106801 (2002)